# Determination of $\pi\pi$ scattering lengths from measurement of $\pi^+\pi^-$ atom lifetime

B. Adeva [a], L. Afanasyev [b], M. Benayoun [c], A. Benelli [d], Z. Berka [e], V. Brekhovskikh [f], G. Caragheorgheopol [g], T. Cechak [e], M. Chiba [h], P.V. Chliapnikov [f], C. Ciocarlan [g], S. Constantinescu [g], S. Costantini [i], C. Curceanu (Petrascu) [g], P. Doskarova [e], D. Dreossi [k], D. Drijard [l,*], A. Dudarev [b], M. Ferro-Luzzi [l], J.L. Fungueiriño Pazos [a], M. Gallas Torreira [l,a], J. Gerndt [e], P. Gianotti [j], D. Goldin [i], F. Gomez [a], A. Gorin [f], O. Gorchakov [b], C. Guaraldo [j], M. Gugiu [g], M. Hansroul [l], Z. Hons [m], R. Hosek [e], M. Iliescu [j,g], V. Karpukhin [b], J. Kluson [e], M. Kobayashi [n], P. Kokkas [o], V. Komarov [b], V. Kruglov [b], L. Kruglova [b], A. Kulikov [b], A. Kuptsov [b], K.I. Kuroda [b], A. Lamberto [p], A. Lanaro [l,q], V. Lapshin [f], R. Lednicky [r], P. Leruste [c], P. Levi Sandri [j], A. Lopez Aguera [a], V. Lucherini [j], T. Maki [s], I. Manuilov [f], J. Marin [t], J.L. Narjoux [c], L. Nemenov [b,l], M. Nikitin [b], T. Nunez Pardo [a], K. Okada [u], V. Olchevskii [b], A. Pazos [a], M. Pentia [g], A. Penzo [v], J.M. Perreau [l], M. Plo [a], T. Ponta [g], G.F. Rappazzo [p], A. Riazantsev [f], J.M. Rodriguez [a], A. Rodriguez Fernandez [a], A. Romero Vidal [j], V.M. Ronjin [f], V. Rykalin [f], J. Saborido [a], C. Santamarina [a], J. Schacher [w], C. Schuetz [i], A. Sidorov [f], J. Smolik [e], F. Takeutchi [u], A. Tarasov [b], L. Tauscher [i], M.J. Tobar [a], T. Trojek [e], S. Trusov [x], V. Utkin [b], O. Vázquez Doce [a], S. Vlachos [i], O. Voskresenskaya [b], T. Vrba [e], C. Willmott [t], V. Yazkov [x], Y. Yoshimura [n], M. Zhabitsky [b], P. Zrelov [b]

[a] *Santiago de Compostela University, Spain*
[b] *JINR Dubna, Russia*
[c] *LPNHE des Universites Paris VI/VII, IN2P3-CNRS, France*
[d] *Zurich University, Switzerland*
[e] *Czech Technical University in Prague, Prague, Czech Republic*
[f] *IHEP Protvino, Russia*
[g] *IFIN-HH, National Institute for Physics and Nuclear Engineering, Bucharest, Romania*
[h] *Tokyo Metropolitan University, Japan*
[i] *Basel University, Switzerland*
[j] *INFN, Laboratori Nazionali di Frascati, Frascati, Italy*
[k] *INFN, Sezione di Trieste and Trieste University, Trieste, Italy*
[l] *CERN, Geneva, Switzerland*
[m] *Nuclear Physics Institute ASCR, Rez, Czech Republic*
[n] *KEK, Tsukuba, Japan*
[o] *Ioannina University, Ioannina, Greece*
[p] *INFN, Sezione di Trieste and Messina University, Messina, Italy*
[q] *University of Wisconsin, Madison, USA*
[r] *Institute of Physics ASCR, Prague, Czech Republic*
[s] *UOEH-Kyushu, Japan*
[t] *CIEMAT, Madrid, Spain* [1]
[u] *Kyoto Sangyo University, Kyoto, Japan*
[v] *INFN, Sezione di Trieste, Trieste, Italy*
[w] *Bern University, Switzerland*
[x] *Skobeltsin Institute for Nuclear Physics of Moscow State University, Moscow, Russia*

## ARTICLE INFO

## ABSTRACT

The DIRAC experiment at CERN has achieved a sizeable production of $\pi^+\pi^-$ atoms and has significantly improved the precision on its lifetime determination. From a sample of 21 227 atomic pairs, a 4% measurement of the S-wave $\pi\pi$ scattering length difference $|a_0 - a_2| = (0.2533^{+0.0080}_{-0.0078}|\mathrm{stat}^{+0.0078}_{-0.0073}|\mathrm{syst})M_{\pi^+}^{-1}$ has been attained, providing an important test of Chiral Perturbation Theory.

## 1. Introduction

Pionium ($A_{2\pi}$) is the $\pi^+\pi^-$ hydrogen-like atom, with 378 fm Bohr radius, which decays predominantly into $\pi^0\pi^0$ [1]. The alternative $\gamma\gamma$ decay accounts for only $\sim 0.4\%$ of the total rate [2]. Its ground-state lifetime is governed by the $\pi\pi$ S-wave scattering lengths $a_I$, with total isospin $I = 0, 2$ [1,3]:

$$\Gamma_{2\pi^0} = \frac{2}{9}\alpha^3 p^\star(a_0 - a_2)^2(1+\delta)M_{\pi^+}^2, \tag{1}$$

where $p^\star = \sqrt{M_{\pi^+}^2 - M_{\pi^0}^2 - (1/4)\alpha^2 M_{\pi^+}^2}$ is the $\pi^0$ momentum in the atom rest frame, $\alpha$ is the fine-structure constant, and $\delta = (5.8 \pm 1.2) \cdot 10^{-2}$ is a correction of order $\alpha$ due to QED and QCD [3] which ensures a 1% accuracy of Eq. (1). The value of $a_0$ and $a_2$ can be rigorously calculated in Chiral Perturbation Theory (ChPT) [4,5], predicting $a_0 - a_2 = (0.265 \pm 0.004)M_{\pi^+}^{-1}$ and the $A_{2\pi}$ lifetime $\tau = (2.9 \pm 0.1) \cdot 10^{-15}$ s [6]. The measurement of $\Gamma_{2\pi^0}$ provides an important test of the theory since $a_0 - a_2$ is sensitive to the quark condensate defining the spontaneous chiral symmetry breaking in QCD [7]. The method reported in this Letter implies observation of the pionium state through its ionization into two pions. Given its large Bohr radius, this is directly sensitive to $\pi\pi$ scattering at threshold, $M_{\pi\pi} \sim 2M_{\pi^+}$, and thus delivers a precision test of the theory without requiring threshold extrapolation, as for semileptonic $Ke4$ decays [8], or substantial theoretical input as for $K \to 3\pi$ decays [9].

## 2. Pionium formation and decay

In collisions with target nuclei, protons can produce pairs of oppositely charged pions. Final-state Coulomb interaction leads to an enhancement of $\pi^+\pi^-$ pairs at low relative c.m. momentum ($Q$) and to the formation of $A_{2\pi}$ bound states or pionium. These atoms may either directly decay, or evolve by excitation (de-excitation) to different quantum states. They would finally decay or be broken up (be ionized) by the electric field of the target atoms. In the case of decay, the most probable channel is $\pi^0\pi^0$ and the next channel is $\gamma\gamma$ with a small branching ratio of 0.36%. In the case of breakup, characteristic atomic pion pairs emerge [10]. These have a very low $Q$ ($< 3$ MeV/$c$) and very small opening angle in the laboratory frame ($< 3$ mrad). A high-resolution magnetic spectrometer ($\Delta p/p \sim 3 \cdot 10^{-3}$) is used [11] to split the pairs and measure their relative momentum with sufficient precision to detect the pionium signal. This signal lays above a continuum background from free (unbound) Coulomb pairs produced in semi-inclusive proton–nucleus interactions. Other background sources are non-Coulomb pairs where one or both pions originate from a long-lived source ($\eta, \eta', \Lambda, \ldots$) and accidental coincidences from different proton–nucleus interactions.

The first observation of $A_{2\pi}$ was performed in the early 1990s [12]. Later, the DIRAC experiment at CERN was able to produce and detect $\sim 6000$ atomic pairs and perform a first measurement of the pionium lifetime [13]. We now present final results from the analysis of $\sim 1.5 \cdot 10^9$ events recorded from 2001 to 2003. Compared to the results in [13], this analysis has reduced systematic errors and improved track reconstruction, mostly due to the use of the GEM-MSGC detector [11] information, which leads to a larger signal yield. The present data come from collisions of 20 and 24 GeV/$c$ protons, delivered by the CERN PS, impinging on a thin Ni target foil of 94 or 98 μm thickness for different run periods.

## 3. Pionium detection and signal analysis

Low relative-momentum prompt and accidental $\pi^+\pi^-$ pairs are produced at the target and selected by the multi-level trigger when their time difference, recorded by the two spectrometer arms, is $|\Delta t| < 30$ ns. A suitable choice of the target material and thickness provides the appropriate balance between the $A_{2\pi}$ breakup and annihilation yields, with reduced multiple-scattering [14,15]. For a thin Ni target, of order $\sim 10^{-3}X_0$, the relative c.m. momentum $Q$ of the atomic pairs is less than $\sim 3$ MeV/$c$ and their number is $\sim 10\%$ of the total number of free pairs in the same $Q$ region [16]. The experiment is thus designed for maximal signal sensitivity in a very reduced region of the $\pi^+\pi^-$ phase space. This is done by selective triggering and by exploiting the high resolution of the spectrometer and background rejection capabilities. The longitudinal ($Q_L$) and transverse ($Q_T$) components of $\vec{Q}$, defined with respect to the direction of the total laboratory momentum of the pair, are measured with precisions 0.55 MeV/$c$ and 0.10 MeV/$c$, respectively.

The double differential spectrum of prompt $\pi^+\pi^-$ pairs $N_{\mathrm{pr}}$ (defined by $|\Delta t| < 0.5$ ns), composed of atomic $n_A$, Coulomb $N_C$, non-Coulomb $N_{\mathrm{nC}}$, and accidental $N_{\mathrm{acc}}$ pairs, can be $\chi^2$-analyzed in the ($Q_T, Q_L$) plane by minimizing the expression

$$\chi^2 = \sum_{ij} \frac{[M^{ij} - F_A^{ij} - F_B^{ij}]^2}{[M^{ij} + (\sigma_A^{ij})^2 + (\sigma_B^{ij})^2]}. \tag{2}$$

Here

$$M(Q_T, Q_L) = \left(\frac{d^2 N_{\mathrm{pr}}}{dQ_T dQ_L}\right)\Delta Q_T \Delta Q_L, \tag{3}$$

and the sum in (2) runs over a two-dimensional grid of $|Q_L| < 15$ MeV/$c$ and $|Q_T| < 5$ MeV/$c$, with bin centres located at values ($Q_T^i, Q_L^j$) and uniform bin size $\Delta Q_T = \Delta Q_L = 0.5$ MeV/$c$. The $F_A$ and $F_B$ functions describe the $A_{2\pi}$ signal and the $N_C + N_{\mathrm{nC}} + N_{\mathrm{acc}}$ three-fold background, respectively; $\sigma_A$ and $\sigma_B$ are their statistical errors. The analysis is based on the parametrization of $F_A$ and $F_B$ and the precise Monte Carlo simulation of the detector response.

The $F_A$ signal has been simulated [17,18] according to an accurate model of $A_{2\pi}$ production, propagation [14], and interaction with the target medium [15,19–21].

In the background $F_B$, the $N_{\mathrm{nC}}$ and the $N_{\mathrm{acc}}$ double differential spectra were parametrized according to two-body phase space and Lorentz boosted to the laboratory frame using the observed pion pair spectra [17]. The spectrum of $N_C$ pairs is enhanced at low $\vec{Q}$

\* Corresponding author.
*E-mail address:* Daniel.Drijard@cern.ch (D. Drijard).
[1] Associated with the university of Santiago de Compostela for technical support in the GEM/MSGC detector.
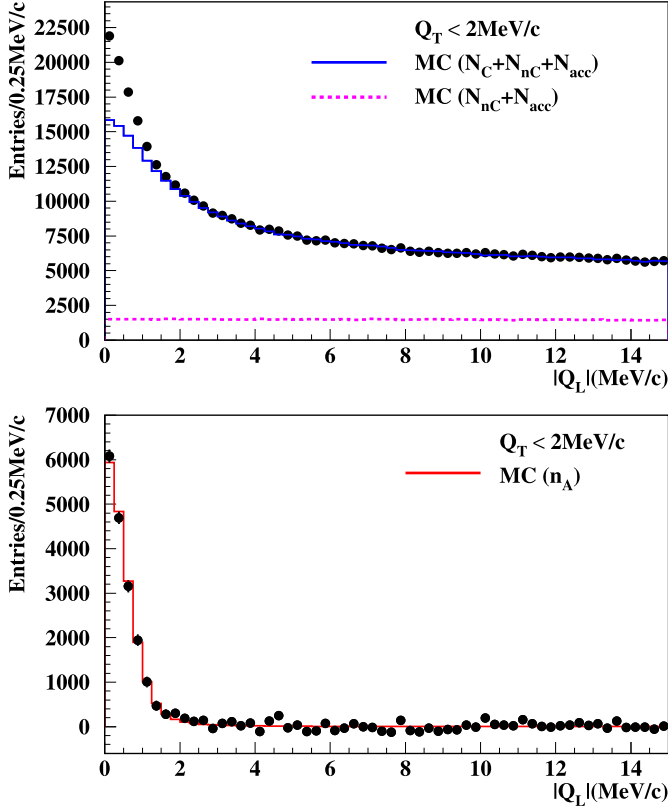
**Fig. 1.** $|Q_L|$ fit projections of the $\pi^+\pi^-$ spectrum from data (dots) and simulation (MC lines). The top plot shows the experimental spectrum compared with the simulated background components (no pionium signal), with (solid line) and without (dotted line) Coulomb pairs ($N_C$). The bottom plot shows the experimental $|Q_L|$ spectrum after background subtraction and the simulated pionium spectrum.

with $Q$ defined at the point of production, by the Coulomb interaction according to the Gamow–Sommerfeld factor

$$A_C(Q) = \frac{2\pi M_\pi \alpha / Q}{1 - \exp(-2\pi M_\pi \alpha / Q)}. \qquad (4)$$

The finite size of the production source and final-state interaction effects have been calculated [22,23] and applied to simulated atomic and Coulomb pairs. An additional momentum-dependent correction has been applied to the simulated $N_C$ spectrum to take into account a small ($< 0.5\%$) contamination, measured by time-of-flight [24], due to misidentified $K^+K^-$ pairs. Small admixtures of misidentified $p\bar{p}$ and residual contamination from $e^+e^-$ pairs have been measured and produce no effect on the final result.

The fraction of accidental pairs in $F_B$ was measured by time-of-flight to be $\omega_{acc} \simeq 12.5\%$, averaged over the pair momentum and the different data sets.

The experimental resolutions on the momentum and opening angle must be accurately simulated in order to extract the narrow pionium signal. Multiple-scattering in the target and the spectrometer is the primary source of uncertainty on the $Q_T$ measurement. In order to achieve the desired $Q_T$ resolution, the scattering angle must be known with $\sim 1\%$ precision, which is beyond the currently available GEANT description [25].

An improved multiple-scattering description was implemented based on dedicated measurements of the average scattering angle off material samples [26]. A cross-check with the standard GEANT description was made by comparing the momentum evolution of the measured distance between $\pi^+$ and $\pi^-$ at the target [27].

The $Q_L$ resolution was checked using $\Lambda$ decays with small opening angle. The widths of reconstructed real and simulated
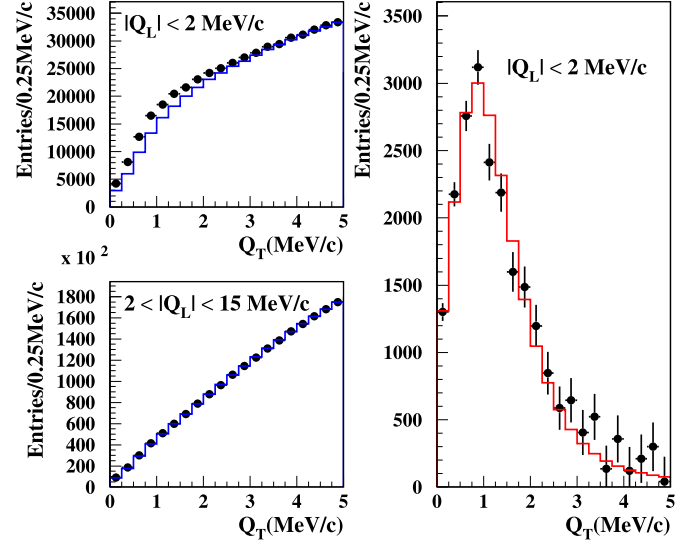


**Fig. 2.** $Q_T$ fit projections of the $\pi^+\pi^-$ spectrum from data (dots) and simulation (line). The left plots show the comparison between the experimental spectra and the full simulated background. The plots correspond to different $Q_L$ regions: top left plot in the $A_{2\pi}$ signal region (low $|Q_L|$) and bottom left plot away from it (higher $|Q_L|$). The right plot shows the $Q_T$ spectrum after background subtraction and the simulated pionium spectrum.
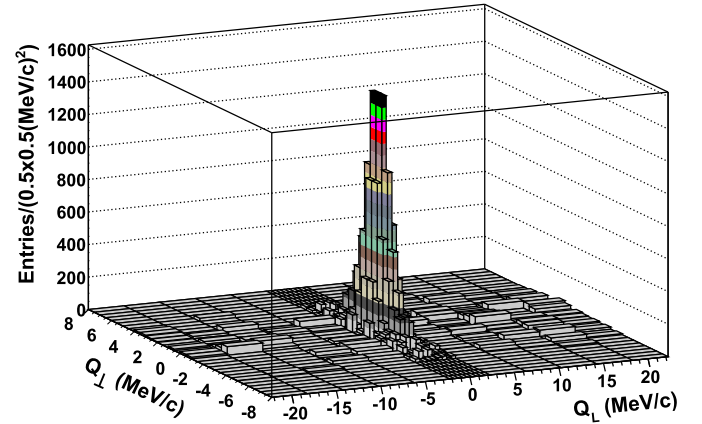


**Fig. 3.** Coulomb subtracted two-pion correlation function measured in the $(Q_\perp, Q_L)$ plane, showing the pionium signal. $Q_\perp$ is the signed projection of $\vec{Q}$ into a generic transverse axis (azimuthal invariance is ensured by the absence of beam and target polarization).

$\Lambda \to p\pi^-$ were compared. A 3.4% relative difference was observed and attributed to residual fringing magnetic field effects, multiple scattering in the downstream vacuum channel exit window, and to a small misalignment between the spectrometer arms. Such effects have been altogether absorbed into an additional Gaussian smearing term, of width $0.66 \cdot 10^{-3}$, convoluted with the simulated momentum resolution function.

The only free parameters in (2) are the number of detected atomic pairs ($n_A^{rec}$) and the fraction of non-Coulomb/Coulomb pairs ($N_{nC}^{rec}/N_C^{rec}$). The minimization is performed in two-dimensional space $|Q_L| < 15$ MeV/c, $Q_T < 5$ MeV/c, for values of the total pair momentum $p$ between 2.6 and 6.8 GeV/c [28]. A constraint on the total number of reconstructed prompt pairs is applied such that $N_{pr}(1 - \omega_{acc}) = N_C^{rec} + N_{nC}^{rec} + n_A^{rec}$.

In Figs. 1 and 2, the $|Q_L|$ and $Q_T$ projections of the experimental prompt $\pi^+\pi^-$ spectrum are shown in comparison to the fitted simulated background spectrum ($F_A = 0$). After subtraction of the $F_B$ background, the experimental $A_{2\pi}$ signal emerges at small

**Table 1**
Fit results for $Q_T < 5$ MeV/$c$ and $|Q_L| < 15$ MeV/$c$.

| Ni, $p_{\text{beam}}$ | $\chi^2$/ndf | $n_A$ | $N_C$ | $N_{nC}$ | $N_{\text{acc}}$ | $P_{\text{br}}$ |
|---|---|---|---|---|---|---|
| 94 µm, 24 GeV/$c$ | 2127/2079 | $6020 \pm 216$ | $546{,}003 \pm 4549$ | $45{,}624 \pm 4501$ | $63{,}212 \pm 208$ | $0.441 \pm 0.018$ |
| 98 µm, 24 GeV/$c$ | 4288/4149 | $9321 \pm 274$ | $828{,}554 \pm 5811$ | $93{,}148 \pm 5754$ | $98{,}499 \pm 255$ | $0.452 \pm 0.015$ |
| 98 µm, 20 GeV/$c$ | 4257/4144 | $5886 \pm 210$ | $496{,}820 \pm 4441$ | $60{,}867 \pm 4397$ | $59{,}392 \pm 144$ | $0.472 \pm 0.020$ |
| Combined samples | | $21{,}227 \pm 407$ | $1{,}871{,}377 \pm 8613$ | $199{,}639 \pm 8526$ | $221{,}103 \pm 359$ | |
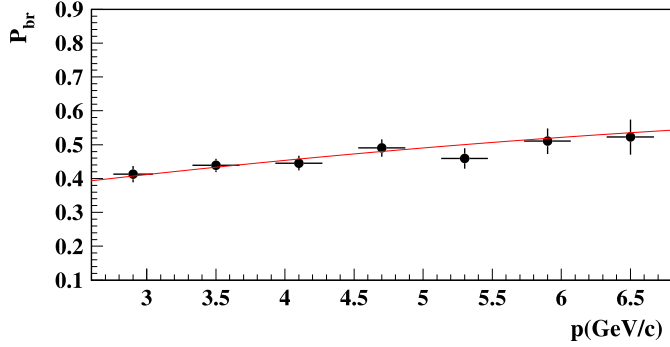


**Fig. 4.** The dependence of the measured $P_{\text{br}}$, averaged over all data sets, from the pionium laboratory momentum and the Monte Carlo prediction corresponding to the ground-state lifetime of $3.15 \cdot 10^{-15}$ s obtained from the best fit.

values of $|Q_L|$ (Fig. 1) and $Q_T$ (Fig. 2) and can be compared with the simulated $F_A$ signal. As expected, multiple-scattering in the target and upstream detectors broadens the $Q_T$ signal shape. This is clearly shown in the 2-dimensional plot of Fig. 3. The overall agreement between the best-fit experimental and simulated spectra is excellent, over the entire $Q_T$, $Q_L$ domain.

## 4. Pionium breakup probability

The pionium breakup probability, $P_{\text{br}}$, is defined as the ratio $n_A/N_A$ between the number $n_A$ of observed pairs from pionium ionization caused by target atoms and the total number $N_A$ of pionium atoms formed by final-state interaction. The latter can be inferred by quantum mechanics from the number of Coulomb-interacting pairs measured at low $Q$ according to the expression [10]

$$\frac{N_A(\Omega)}{N_C(\Omega)} = \frac{(2\pi M_\pi \alpha)^3}{\pi} \cdot \frac{\sum_{n=1}^{\infty} 1/n^3}{\int_\Omega A_C(Q) d^3 Q} = K^{\text{th}}(\Omega), \qquad (5)$$

where $\Omega$ is the domain of integration $|Q_L| < 2$ MeV/$c$ and $Q_T < 5$ MeV/$c$, yielding $K^{\text{th}} = 0.1301$. Differences in detector acceptance and reconstruction efficiency for $n_A$ and $N_C$ pairs, $\epsilon_A$ and $\epsilon_C$ respectively, are taken into account by correcting the theoretical factor $K^{\text{th}}$ as

$$K^{\text{exp}}(\Omega) = K^{\text{th}}(\Omega) \frac{\epsilon_A(\Omega)}{\epsilon_C(\Omega)}. \qquad (6)$$

Those differences arise mainly from the lesser resolution of the upstream detectors for identifying close tracks at very low $Q_T$. This occurs more frequently for atomic pairs than for Coulomb pairs.

The breakup probability is thus determined as

$$P_{\text{br}} = \frac{n_A}{N_A} = \frac{n_A^{\text{rec}}(\Omega)}{N_C^{\text{rec}}(\Omega)} \cdot \frac{1}{K^{\text{exp}}(\Omega)}. \qquad (7)$$

The momentum-dependent $K^{\text{exp}}$ factor (6) has been calculated from fully reconstructed Monte Carlo atomic and Coulomb pairs. Using (6) and (7), 35 independent $P_{\text{br}}$ values are obtained for the five independent data sets and for seven 600 MeV/$c$ wide bins
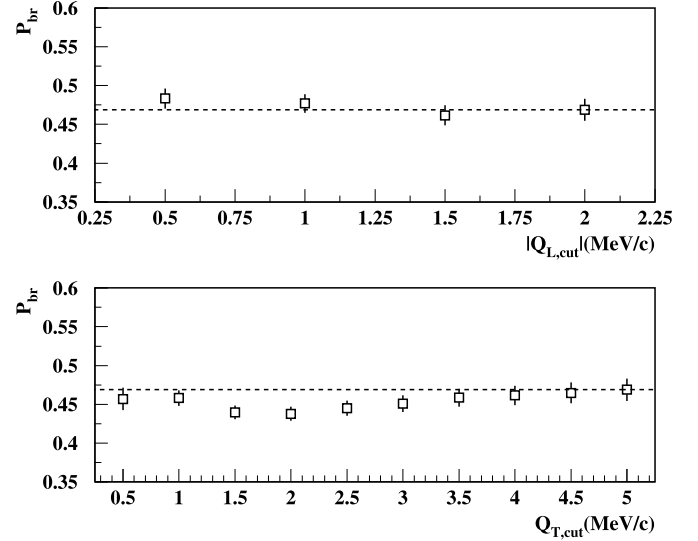


**Fig. 5.** Stability of the average $P_{\text{br}}$ with respect to variation of the: (top) $|Q_L|$ (for $Q_T < 5$ MeV/$c$ ) and (bottom) $Q_T$ (for $|Q_L| < 2$ MeV/$c$) integration limits, in 0.5 MeV/$c$ bins.

of the $A_{2\pi}$ momentum from 2.6 to 6.8 GeV/$c$, by appropriately folding the momentum dependence of $K^{\text{exp}}$.

In Table 1 the fitted yields are given for the different momentum-averaged data sets. Overall, more than $2 \cdot 10^4$ atomic pairs have been detected. The reported $P_{\text{br}}$ values are only indicative of the amount of variation expected with respect to the different experimental conditions, and they are not used in the final momentum-dependent fit.

A slight increase of the measured $P_{\text{br}}$ with increasing pionium momentum is observed in Fig. 4 (data points), which is a consequence of the longer decay path, and hence the greater breakup yield, expected at higher atom momenta. The continuous curve represents the predicted evolution of $P_{\text{br}}$ with pionium laboratory momentum, for the value of the pionium ground-state lifetime $\tau = 3.15 \cdot 10^{-15}$ s obtained from this analysis.

The dependence of the $A_{2\pi}$ breakup probability on the specific choice of the integration domain $\Omega$ has been verified. The measured $P_{\text{br}}$, averaged over the data sets, is indeed very stable versus variations of the $|Q_L|$, $Q_T$ integration limits as shown in Fig. 5.

## 5. Results and systematic errors

A detailed assessment of the systematic errors affecting the $P_{\text{br}}$ measurement has been carried out, considering all known sources of uncertainty in the simulation and in the theoretical calculations. The largest systematic error comes from a $\sim 1\%$ uncertainty in the multiple-scattering angle inside the Ni target foil which induces a $\pm 0.0077$ error on $P_{\text{br}}$. The momentum smearing correction can increase $P_{\text{br}}$ by $\sim 2\%$ and thus produce a $\pm 0.0026$ systematic error. The double-track resolution at small angles can change $P_{\text{br}}$ by 1.1% and generate a systematic error of $\pm 0.0014$. The admixture of $K^+K^-$ changes $P_{\text{br}}$ by $\sim 1\%$. The uncertainty

**Table 2**
Summary of systematic errors on $P_{br}$.

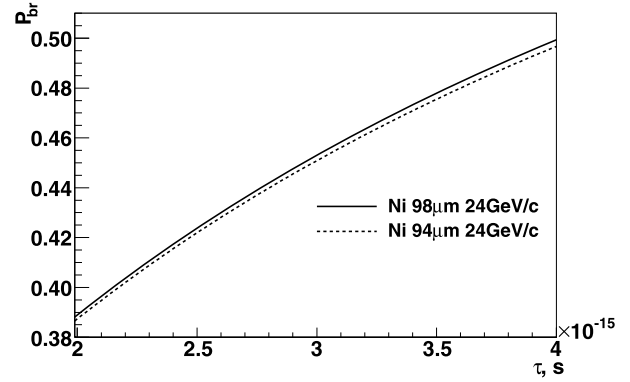| Source | $\sigma$ |
| --- | --- |
| multiple scattering | $\pm 0.0077$ |
| momentum smearing | $\pm 0.0026$ |
| double-track resolution | $\pm 0.0014$ |
| $K^+K^-$ and p$\bar{p}$ | $\pm 0.0011$ |
| trigger simulation | $\pm 0.0004$ |
| background hits | $\pm 0.0001$ |
| target impurity | $\pm 0.0013$ |
| finite size | $\pm 0.0011$ |
| calculation of $P_{br}(\tau)$ | $\pm 0.0042$ |
| Overall error | $\pm 0.0094$ |



**Fig. 6.** Function $P_{br}(\tau)$ corresponding to the dependence on pionium lifetime of the breakup probability for different targets.

on such contamination is 15% and produces a systematic error of $\pm 0.0011$ on $P_{br}$. The finite-size correction to the point-like approximation creates a maximum 0.8% variation of the simulated yield of Coulomb pairs and a systematic error of $\pm 0.0011$ on $P_{br}$. The influence of the final-state strong interaction on the $\tau$ dependence of $P_{br}$ is negligible [18,22]. The trigger response efficiency was measured using minimum-bias events and accidental pairs from calibration runs. The efficiency is high and quite uniform in the selected $Q_T$, $Q_L$ domain and it drops by $\sim 2\%$ per MeV/$c$ at $|Q_L| > 15$ MeV/$c$. The simulated and experimental trigger efficiencies agree to better than 0.5%, in the same $|Q_L|$ range. This maximum deviation increases the breakup probability by $\sim 3\%$ and thus produces a systematic error of $\pm 0.0004$. Background hits in the upstream spectrometer region, generated by beam and secondary interactions in the target region, are the source of a $\pm 0.0001$ systematic error on $P_{br}$. The effect of the lower purity of the 94 μm Ni target foil compared to the 98 μm is an underestimation of $P_{br}$ by $\sim 1.1\%$. This corresponds to a systematic error of $\pm 0.0013$ for the corresponding data set.

The dependence of $P_{br}$ on the atom lifetime $\tau$, its momentum, and the target parameters has been extensively studied for several target materials, both by exactly solving the system of transport equations [14,18] describing the $A_{2\pi}$ excitation/de-excitation, breakup and annihilation, and by simulating [15] the $A_{2\pi}$ propagation in the target foil. The precision reached by these calculations is at the level of 1% [29], which is reflected in a $\pm 0.0042$ systematic error on $P_{br}$ for a lifetime $\tau = 3.15 \cdot 10^{-15}$ s. The result of these calculations defines three functions $P_{br}(\tau, p)$, one for each of the combinations of target thickness and beam momentum. The functions $P_{br}(\tau, p)$ are further convoluted with the experimental momentum spectra of Coulomb pairs inside the seven (600 MeV/$c$ wide) momentum slices of the pionium laboratory momentum, from 2.6 to 6.8 GeV/$c$. This approach ensures that within each slice the non-linear dependence of $P_{br}(\tau)$ on the laboratory momentum is negligible.

Coulomb pairs, which have a momentum spectrum similar to that of atomic pairs, are taken from prompt pairs in the $\vec{Q}$ region away from the $A_{2\pi}$ signal, after subtraction of the non-Coulomb contribution. The values of the systematic errors are summarized in Table 2.

## 6. Conclusions

Finally, the $P_{br}$ measurements, obtained for the different experimental conditions and $A_{2\pi}$ momentum ranges, and their predicted $P_{br}(\tau, p)$ values (see Fig. 6), were used in a maximum likelihood fit of the lifetime $\tau$ [30]. Both statistical and systematic uncertainties were taken into account in the maximization procedure.

Our final measurement of the ground-state $A_{2\pi}$ lifetime yields $\tau = (3.15^{+0.20}_{-0.19}|_{stat}{}^{+0.20}_{-0.18}|_{syst}) \cdot 10^{-15}$ s.

Taking into account $A_{2\pi} \to \gamma\gamma$ and using formula (1), we obtain the $\pi\pi$ scattering length difference

$$|a_0 - a_2| = \left(0.2533^{+0.0080}_{-0.0078}|_{stat}{}^{+0.0078}_{-0.0073}|_{syst}\right)M_{\pi^+}^{-1}, \qquad (8)$$

where the systematic error includes the 0.6% uncertainty induced by the theoretical uncertainty on the correction $\delta$.

In conclusion, we have measured the ground-state lifetime of pionium with a total uncertainty of $\sim 9\%$. This represents the most accurate lifetime measurement ever obtained and has allowed us to determine the scattering length difference $|a_0 - a_2|$ with a $\sim 4\%$ accuracy. Our result is in agreement with values of the scattering lengths obtained from $K_{e4}$ [8] and $K_{3\pi}$ [9] decay measurements using a completely different experimental approach.

## Acknowledgements

## References

[1] J. Uretsky, J. Palfrey, Phys. Rev. 121 (1961) 1798.
[2] J. Gasser, et al., Phys. Rep. 456 (2008) 167.
[3] J. Gasser, et al., Phys. Rev. D 64 (2001) 016008.
[4] S. Weinberg, Physica A 96 (1979) 327.
[5] J. Gasser, H. Leutwyler, Nucl. Phys. B 250 (1985) 465.
[6] G. Colangelo, et al., Nucl. Phys. B 603 (2001) 125.
[7] M. Knecht, et al., Nucl. Phys. B 457 (1995) 513.
[8] J.R. Batley, et al., Eur. Phys. J. C 70 (2010) 635;
    G. Colangelo, J. Gasser, A. Rusetsky, Eur. Phys. J. C 59 (2009) 777.
[9] J.R. Batley, et al., Eur. Phys. J. C 64 (2009) 589;
    G. Colangelo, et al., Phys. Lett. B 638 (2006) 187.
[10] L.L. Nemenov, Sov. J. Nucl. Phys. 41 (1985) 629.
[11] B. Adeva, et al., Nucl. Instrum. Meth. A 515 (2003) 467.
[12] L.G. Afanasyev, et al., Phys. Lett. B 338 (1994) 478.
[13] B. Adeva, et al., Phys. Lett. B 619 (2005) 50.
[14] L.G. Afanasyev, A.V. Tarasov, Phys. At. Nucl. 59 (1996) 2130.
[15] C. Santamarina, et al., J. Phys. B 36 (2003) 4273.
[16] O.E. Gorchakov, et al., Phys. At. Nucl. 59 (1996) 1942.
[17] M.V. Zhabitsky, DIRAC notes 2007-01, 2007-11, http://cdsweb.cern.ch/record/1369660.
[18] M.V. Zhabitsky, Phys. At. Nucl. 71 (2008) 1040.
[19] L. Afanasyev, et al., J. Phys. G 25 (1999) B7.
[20] L. Afanasyev, et al., Phys. Rev. D 65 (2002) 096001.
[21] M. Schumann, et al., J. Phys. B 35 (2002) 2683.

[22] R. Lednicky, J. Phys. G: Nucl. Part. Phys. 35 (2008) 125109.
[23] P.V. Chliapnikov, V.M. Ronjin, J. Phys. G: Nucl. Part. Phys. 36 (2009) 105004.
[24] B. Adeva, et al., DIRAC note 2007-02, http://cdsweb.cern.ch/record/1369659.
[25] G.R. Lynch, O.I. Dahl, Nucl. Instrum. Meth. B 58 (1991) 6.
[26] A. Dudarev, et al., DIRAC note 2008-06, http://cdsweb.cern.ch/record/1369639.

[27] B. Adeva, et al., DIRAC note 2005-16, http://cdsweb.cern.ch/record/1369675.
[28] B. Adeva, et al., DIRAC note 2006-03, http://cdsweb.cern.ch/record/1369664.
[29] A.V. Tarasov, I.U. Khristova, JINR-P 2-91-10 (1991).
[30] D. Drijard, M. Zhabitsky, DIRAC note 2008-07, http://cdsweb.cern.ch/record/1369638.